*Present address: 1615 W. Catalpa, Chicago, Ill. 60640.

[1]I. M. Tang, Phys. Rev. B **2**, 3592 (1970).

[2]Interaction Hamiltonian is written in the mean field approximation of the Suhl-Matthias-Walker Hamiltonian:

$$\mathcal{H} = \sum_\sigma \int \left[(2m_s)^{-1} \nabla\psi_{s\sigma}^\dagger \nabla\psi_{s\sigma} + \frac{1}{2m_d} \nabla\psi_{d\sigma}^\dagger \nabla\psi_{d\sigma} \right] d^3r$$
$$+ c\sum_\sigma \int (\psi_{s\sigma}^\dagger \psi_{s\sigma} + \psi_{d\sigma}^\dagger \psi_{d\sigma})\, \phi\, d^3r - g_s \int \psi_{s\uparrow}^\dagger \psi_{s\downarrow}^\dagger \psi_{s\downarrow} \psi_{s\uparrow}\, d^3r$$
$$- g_d \int \psi_{d\uparrow}^\dagger \psi_{d\downarrow}^\dagger \psi_{d\downarrow} \psi_{d\uparrow}\, d^3r - g_{sd} \int \{ \psi_{s\uparrow}^\dagger \psi_{s\downarrow}^\dagger \psi_{d\downarrow} \psi_{d\uparrow}$$
$$+ \psi_{d\uparrow}^\dagger \psi_{d\downarrow}^\dagger \psi_{s\downarrow} \psi_{s\uparrow} \} d^3r.$$

[3]See, for instance, Y. B. Kim and M. T. Stephen, in *Treatise on Superconductivity*, edited by R. D. Parks (Dekker, New York, 1969).

[4]C. Caroli and K. Maki, Phys. Rev. **164**, 591 (1967).

[5]K. Maki, Progr. Theoret. Phys. (Kyoto) **41**, 902 (1969).

[6]H. Suhl, B. T. Matthias, and L. R. Walker, Phys. Rev. Letters **3**, 552 (1959).

[7]J. W. Hafstrom, R. M. Rose, and M. L. A. MacVicar, Phys. Letters **30A**, 379 (1969).

[8]J. R. Calrson and C. B. Satterthwaite, Phys. Rev. Letters **24**, 461 (1970).

[9]R. Radebaugh and P. H. Keesom, Phys. Rev. **149**, 209 (1966).

[10]L. Y. L. Shen, N. M. Senozan, and N. E. Phillips, Phys. Rev. Letters **14**, 1025 (1965).

[11]C. C. Sung and L. Y. L. Shen, Phys. Letters **19**, 101 (1965).

[12]V. Radhakrishnan, Phys. Status Solidi **20**, 783 (1967).

[13]B. W. Maxfield and W. L. McLean, Phys. Rev. **139**, A1515 (1965).

[14]Both the electric-current and the heat-current operators in the SMW model are of this type.

[15]J. Bardeen and M. J. Stephen, Phys. Rev. **140**, A1197 (1965).

[16]P. Noziéres and W. F. Vinen, Phil. Mag. **14**, 667 (1967).

[17]Y. B. Kim, C. F. Hempstead, and A. R. Strand, Phys. Rev. **139**, A1163 (1965).

[18]A. Schmid, Physik Kondensierten Materie **5**, 302 (1966).

[19]J. W. Garland, Phys. Rev. Letters **19**, 227 (1967).

[20]J. Gusman, J. Phys. Chem. Solids **28**, 2327 (1967).

[21]S. M. Wasim and N. H. Zebouni, Phys. Rev. **187**, 539 (1969).

[22]R. P. Huebener, R. T. Kampwirth, and A. Seher, J. Low Temp. Phys. **2**, 113 (1970).

[23]A. T. Firoy and B. Serin, Phys. Rev. Letters **21**, 359 (1968).

[24]It can be easily shown that the two-band heat-current operator satisfies the heat equation $\partial/\partial t\, h(r) + \nabla \cdot \mathbf{j}^{(h)}(r) = 0$, where $h(r)$ is the Hamiltonian density in the SMW model.

Tunneling into Weakly Coupled Films of Aluminum and Tin in Proximity*

J. Vrba and S. B. Woods

Department of Physics, University of Alberta, Edmonton 7, Canada

(Received 24 August 1970)

Tunneling experiments have been performed into the N side of N-S (aluminum-tin) proximity sandwiches evaporated at room temperature onto an oxidized aluminum electrode B. The coupling between the N and S films was made weak by allowing slight oxidation to occur at the interface. When B is normal, the normalized tunneling conductance of these junctions in the vicinity of the critical temperature of the proximity sandwich is markedly different from that of junctions formed between B and an ordinary (BCS) superconductor. When B is superconducting and the thickness of the N film is made about $d_N \simeq 100$ Å $\simeq \frac{1}{10} d_S$, where d_S is the thickness of the S film, a double-peaked structure is observed in the tunnel conductance as a function of applied voltage. The properties of the proximity sandwich depend on the amount of oxidation at the N-S interface. Self-consistent calculations have been performed using the McMillan model of proximity sandwiches and treating the barrier transmission as a parameter. Comparison of these calculations with the experimental results shows satisfactory quantitative agreement.

INTRODUCTION

Recently a simple theoretical model of the proximity effect between superposed normal (N) and superconducting (S) metal films has been proposed by McMillan[1] and calculations of the transition temperature, energy gap, and electronic density of states were made for comparison with the results of tunneling experiments. He treats, by second-order self-consistent perturbation theory, a model

in which thin metal films are coupled by tunneling through a barrier at the interface. Experiments by Adkins and Kington[2] and by Freake and Adkins[3] showed reasonable agreement with general features of the theory, which is as much as could be expected, since their films were rather strongly coupled and the theory only applies strictly to weak coupling between the two films.

The coupling may be weakened by allowing a very thin oxide layer with an electron transmission prob-

ability α to form at the interface. We have observed an interesting double-peaked structure in the differential conductance as a function of bias voltage for tunnel currents from a superconductor into the N side of a weakly coupled N-S-layered sandwich composed of aluminum and tin. When the thickness of the N film is made about $d_N \simeq 100$ Å $\simeq \frac{1}{10} d_S$, where d_S is the thickness of the S film, the double-peaked structure is observed and at the same time the properties of the N-S structure are very dependent on the value of α. For thicker N films, for which some results have been reported,[4] the double-peaked structure disappears and the α dependence diminishes. Tunneling from a normal metal into these weakly coupled thin aluminum-tin proximity sandwiches provides evidence over a broad range of film thickness and mean free path for the empirical relationship connecting zero-bias conductance and temperature proposed by Guyon et al.[5] Tunneling results from both a normal metal and superconductor into the aluminum-tin proximity films are interpreted in terms of McMillan's theory, with which a satisfactory quantitative agreement may be obtained.

EXPERIMENTAL

The tunnel junctions were prepared at room temperature in a metal evaporator He[4] cryostat[6,7] by first evaporating a base layer of aluminum through a mask with a slit $\frac{1}{16}$ in. wide onto a glass substrate and oxidizing it to form a tunnel barrier; the proximity sandwiches were then evaporated as cross strips also $\frac{1}{16}$ in. wide over the oxidized aluminum. The sandwich consisted of a thin aluminum layer that was allowed to oxidize very slightly and then a thicker tin layer that was evaporated onto its exposed surface. The source-to-substrate distance during evaporation was about 17 in., so that the film thicknesses were uniform over the whole specimen area and the vacuum was better than 10^{-7} Torr before evaporations were started and did not exceed 10^{-6} Torr during evaporation. The aluminum was evaporated from a stranded tungsten wire that was frequently renewed and the tin from a tantalum boat.

The base layer was oxidized using a glow discharge[8] for about 350 sec in a dry oxygen atmosphere at a pressure of ~0.15 Torr. The glow electrode was a 2-in.-diam ring of aluminum wire located about 3 in. from the substrate. The electrode was maintained at a negative potential of ~350 V and the glow current was 1 mA. These conditions would produce a junction resistance of ~100 Ω if the aluminum of the proximity sandwich was evaporated within a few minutes and was at least 100 Å thick. Thinner layers required less oxidation time to produce the same resistance, whereas a delay of about 2 h before evaporating the aluminum cover layer necessitated twice the oxidation time.

The thickness of the films was measured with a quartz-crystal monitor calibrated with a Tolansky interferometer. For the monitor, we have measured the beat frequency of two AT-cut quartz crystals mounted in the same water-cooled copper holder, so that one crystal was exposed to the evaporating metal and the other only to the heat change during evaporation. Such temperature compensation reduced by more than a factor of 2 the frequency shift that was induced by the heat from the evaporation source when thick films were deposited.

The vacuum was maintained in the specimen chamber from the time the samples were manufactured until measurements were completed at liquid-helium temperatures. The samples were cooled to liquid-nitrogen temperatures within 30 min after the final evaporation and were held there if extended waits were necessary. Although interdiffusion may often occur in proximity sandwiches, the solid solubilities for the aluminum-tin system are very restricted and no intermetallic compounds are known[9]; also, a slight oxide was formed between the aluminum and tin which would further reduce diffusion effects. Perhaps the strongest evidence that our procedures produced proximity structures with distinct aluminum and tin films lies in the tunneling results which exhibit several characteristics that would not arise in a badly interdiffused or alloyed structure.[5]

THEORETICAL BACKGROUND

Difficulties arise in calculating the superconducting properties of normal-metal–superconductor (N-S) sandwiches because in such a system the order parameter is space dependent, and solutions have been obtained only in the vicinity of the critical temperature T_c.[10] McMillan avoids this problem by assuming that each metal is sufficiently thin that the superconducting properties are constant across it and he is then able to obtain a complete solution for this model valid for all temperatures $T < T_c$.

McMillan's Model

The following assumptions are made about the experimental system.

(a) A film of superconductor S of thickness d_S is separated by a potential barrier with electron transmission probability α from a film of normal metal N (or different superconductor) with thickness d_N.

(b) The tunneling Hamiltonian is used to describe the penetration of electrons through the barrier, which restricts the transmission probability α to be much less than 1.

(c) Both N and S are thin compared with the coherence length.

(d) The ratio of the mean free path l to the film

thickness is greater than unity.

Using this model, McMillan has derived the simultaneous self-energy equations for fixed BCS potentials Δ_S^{ph} and Δ_N^{ph} (in films S and N, respectively) to be

$$\Delta_N(E) = \left(\Delta_N^{ph} + \frac{i\Gamma_N \Delta_S(E)}{[E^2 - \Delta_S^2(E)]^{1/2}}\right) \Big/$$

$$\left(1 + \frac{i\Gamma_N}{[E^2 - \Delta_S^2(E)]^{1/2}}\right) ,$$

$$(1)$$

$$\Delta_S(E) = \left(\Delta_S^{ph} + \frac{i\Gamma_S \Delta_N(E)}{[E^2 - \Delta_N^2(E)]^{1/2}}\right) \Big/$$

$$\left(1 + \frac{i\Gamma_S}{[E^2 - \Delta_N^2(E)]^{1/2}}\right) .$$

The self-consistency conditions for the BCS potentials at temperature T are[11]

$$\Delta_N^{ph} = \lambda_N \int_A^B \text{Re}\left(\frac{\Delta_N(E)}{[E^2 - \Delta_N^2(E)]^{1/2}}\right) \tanh\frac{E}{2kT} dE ,$$

$$(2)$$

$$\Delta_S^{ph} = \lambda_S \int_C^D \text{Re}\left(\frac{\Delta_S(E)}{[E^2 - \Delta_S^2(E)]^{1/2}}\right) \tanh\frac{E}{2kT} dE ,$$

and the electronic density of states can be computed from

$$N_{S,N} = \text{Re}\{|E| / [E^2 - \Delta_{S,N}^2(E)]^{1/2}\} .$$

$$(3)$$

In the above equations Γ_S and Γ_N fulfill the corrected[12] conditions

$$\Gamma_N = \pi\mathcal{T}^2 A d_S N_S(0) = \hbar/2\tau_N ,$$

$$\Gamma_S = \pi\mathcal{T}^2 A d_N N_N(0) = \hbar/2\tau_S ,$$

where $\mathcal{T}$ is the tunneling matrix element, A is the area of the junction, $N_{N,S}(0)$ is the density of states at the Fermi level, and $\tau_{N,S}$ are the relaxation times in the normal and superconducting material, respectively.

We may write

$$\tau_{N,S} = L_{N,S}/v_{FN,S}\alpha ,$$

where $v_{FN,S}$ is the Fermi velocity and $L_{N,S}$ is the average electron path length between collisions with the barrier in the N or S film, respectively.

$L_{N,S} = 4d_{N,S}$ if the following conditions are fulfilled: (a) The mean free path $l_{N,S}$ is infinite and (b) the probability that an electron penetrates the barrier to enter the film at an angle θ to the normal obeys the cosine law. For a film which does not fulfill these conditions, we may write

$$L_{N,S} = 2B_{N,S}(l_{N,S}/d_{N,S})d_{N,S} ,$$

where B is a function of the ratio of the mean free path to the film thickness. Also, we can write

$$\Gamma_N = \frac{\hbar v_{FN}\alpha}{4B_N d_N} , \quad \Gamma_S = \frac{\hbar v_{FS}\alpha}{4B_S d_S} . \quad (4)$$

A maximum practical value for these parameters is $\Gamma \simeq 10$ meV. This is obtained with $d \simeq 15$ Å (where our films became continuous), $v_F \simeq 10^8$ cm/sec, $B_N = 2$, and $\alpha \simeq 0.1$.

Calculations for Aluminum-Tin Sandwich

We have carried out detailed computer calculations for the aluminum-tin proximity sandwich with an analysis of the tunneling density of states in the aluminum film. The results are presented here in graphical form. We refer to aluminum as the normal metal (even when it is superconducting) and tin is the superconductor.

An interesting feature of McMillan's model is the double-peaked density of states that appears when $d_N < d_S$ ($\Gamma_S/\Gamma_N < 1$) and α is small. The exact shape and energy of the peaks depends on the parameters Γ_S, Γ_N, Δ_S^{ph}, and Δ_N^{ph}. When d_N approaches d_S ($\Gamma_S/\Gamma_N \to 1$) or α is increased, the density of states exhibits a broad single peak. The situation in the N film is illustrated in Fig. 1 for two different values of α, with the simplifying conditions $B_N = B_S = 2$, $v_{FN} = v_{FS} = 10^8$ cm/sec, $\Delta_S^{ph} = 1.0$ meV, and $\Delta_N^{ph} = 0.1$ meV. A double-peaked structure also exists in the S film, but all considerations here are restricted to the N film.

The appearance of the double-peaked structure may be understood qualitatively in terms of two effects that the presence of the tin has on the aluminum. First, the wave functions of the excitations in the tin are coupled into the aluminum, creating a peak in the density of states near Δ_S^{ph}; second, as α increases, the pairing energies in the two metals
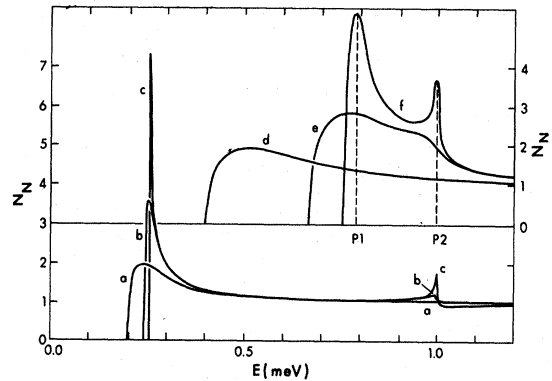

FIG. 1. McMillan's density of states in the N side of a proximity sandwich at fixed values of the potentials $\Delta_S^{ph} = 1.0$ meV, $\Delta_N^{ph} = 0.1$ meV. $B_N = B_S = 2$, $v_{FN} = v_{FS} = 10^8$ cm sec^{-1}, $d_N = 60$ Å for all curves. $d_S = 60$ Å for curves a, d; $d_S = 600$ Å for b, c; $d_S = 6000$ Å for e, f. $\alpha = 0.005$ for a-c; $\alpha = 0.05$ for d-f. For higher α the peaks are closer together and larger d_S is required to resolve the double-peaked structure.

move toward a common value determined largely by the thicker metal. Thus for $d_S > d_N$ the low-energy excitation peak in aluminum moves to higher energies as α increases, and also the eigenstates of the system become less well defined, so that the peaks gradually broaden and merge.

The temperature variation of the peak positions and of the BCS potentials Δ_S^{ph} and Δ_N^{ph} can be calculated by combining the self-energy equation (1) with the self-consistent condition expressed by Eq. (2). For aluminum and tin the bulk values $\lambda_N = 0.171$, $\omega_c^N = 32.21$ meV, $\lambda_S = 0.246$, and $\omega_c^S = 16.78$ meV were substituted; also, $\Gamma_S/\Gamma_N = 0.1$, $d_N = 60$ Å, $d_S = 600$ Å, $B_N = B_S = 2$, $v_{FN} = v_{FS} = 1 \times 10^8$ cm/sec, and the values $\alpha = 0.02$, 0.002, 0.0002 were used. It can be seen from Fig. 2 that for weak coupling between the films (case a) the higher-energy peak $P2 \simeq \Delta_S^{ph}$ follows closely the BCS temperature variation of the tin gap, while the lower-energy peak $P1$ and Δ_N^{ph} at low temperature follow the BCS temperature dependence for the aluminum gap, but deviate progressively as the temperature is raised and finally approach zero at T_c of the over-all sandwich. As the interaction between the films is made stronger (cases b and c in that order), the value of $P2 \simeq \Delta_S^{ph}$ is lowered for all temperatures, while $P1$ and Δ_N^{ph} are shifted to higher energies.

The temperature dependence of Δ_S^{ph} in each case is well approximated by the BCS relationship for $\Delta(T)/\Delta(T=0)$, so that the critical temperature T_c of the sandwich may be found from the relation[13]

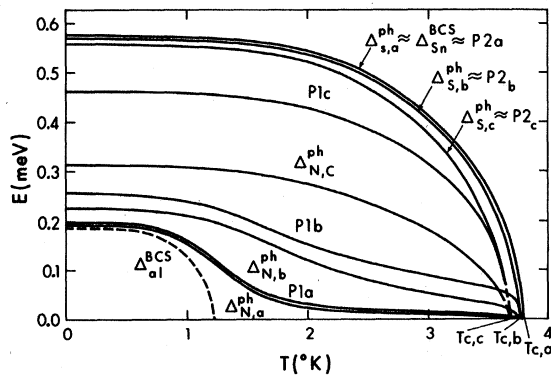$$2\Delta_S^{ph}(T=0)/kT_c \simeq 3.5 \ . \tag{5}$$

FIG. 2. Temperature variation of the self-consistently determined potentials Δ_S^{ph} and Δ_N^{ph} and peaks $P1$ and $P2$ in the density states. Bulk value $\omega_c^N = 32.21$ meV, $\lambda_N = 0.171$ were used for aluminum; $\omega_c^S = 16.78$ meV, $\lambda_S = 0.246$ for tin. $\Gamma_S/\Gamma_N = 0.1$ for all curves, $\Gamma_N = 0.005$ meV for a, $\Gamma_N = 0.05$ meV for b, $\Gamma_N = 0.5$ meV for c. Δ_S^{ph} is usually indistinguishable from $P2$. BCS variation of the tin gap is indistinguishable from Δ_{Sa}^{ph}. Dashed curve, BCS variation of the aluminum gap. $T_c = 3.80$ °K for a, $T_c = 3.77$ °K for b, $T_c = 3.69$ °K for c. These critical temperatures were obtained using Eq. (5).

When self-consistent values of Δ_N^{ph} and Δ_S^{ph}, peak positions, and peak separations are plotted aginst Γ_N for different ratios Γ_S/Γ_N, one finds a very important result. The properties of the system shown in Figs. 3(a)–3(c) are independent of Γ_S (and therefore of B_S or d_S) over a wide range of Γ_N. This feature is used for evaluation of our experimental data. In Fig. 3(d), Δ_S^{ph} and Δ_N^{ph} are shown as functions of Γ_S for different ratios of Γ_S/Γ_N to emphasize that these properties are much more dependent on Γ_N than on Γ_S.

The region in which the double peak may be experimentally observed is estimated to be

$$0.005 \lesssim \Gamma_N \lesssim 1.0 \ \text{meV} \ . \tag{6}$$

The lower limit is determined by the magnitude of $P2$ (see Fig. 1), which becomes smaller as Γ_N is decreased, while the upper limit is approximately the point where the two peaks merge as may be determined from Fig. 3(b). From Eq. (4), using $v_{FN} = 10^8$ cm/sec and $B_N = 2$, Eq. (6) becomes

$$6 \times 10^{-6} \lesssim \alpha/d_N \lesssim 10^{-3} \ ,$$

where d_N is expressed in Å.

TUNNELING INTO N SIDE OF PROXIMITY SANDWICH

The normalized differential conductance $\sigma(V)$ of a tunnel junction formed between two metals A and B can be expressed in terms of their normalized densities of electronic states N_A and N_B (assuming constant tunneling matrix elements) by the expression

$$\sigma(V) = \frac{(dI/dV)_S}{(dI/dV)_N} = \int_{-\infty}^{+\infty} N_A(E) \left(\frac{\partial N_B(E - V)}{\partial V} \phi(E, V) \right.$$
$$\left. + N_B(E - V) \frac{\partial \phi(E, V)}{\partial V} \right) dE \ , \tag{7}$$

where E is energy, V is the applied voltage in energy units, and

$$\phi(E, V) = [1 + e^{(E-V)/kT}]^{-1} - [1 + e^{E/kT}]^{-1} \ .$$

In order to carry out numerical calculations the functions N_A, N_B, and the derivative $\partial N_B/\partial V$ must be finite. We have used the approximation

$$N_B = 1 \qquad\qquad \text{if } B \text{ is a normal metal}$$
$$= \text{Re}[\, |E| \, /(E^2 - \Delta^2)^{1/2}] \quad \text{if } B \text{ is a superconductor,} \tag{8}$$

where $\Delta = \Delta_B(1 + i\delta)$, with Δ_B the BCS energy gap in metal B. N_A is the McMillan density of states for the N film of the proximity sandwich.

The constant δ has been evaluated by fitting Eq. (7) to experimental tunneling data. $\delta_{A1} = 0.013$ was obtained by putting $N_A = N_B = N_{A1}$ and fitting to data for an Al-I-Al junction at $T = 0.4$ °K; then, using this value, Eq. (7) was again fitted to results for
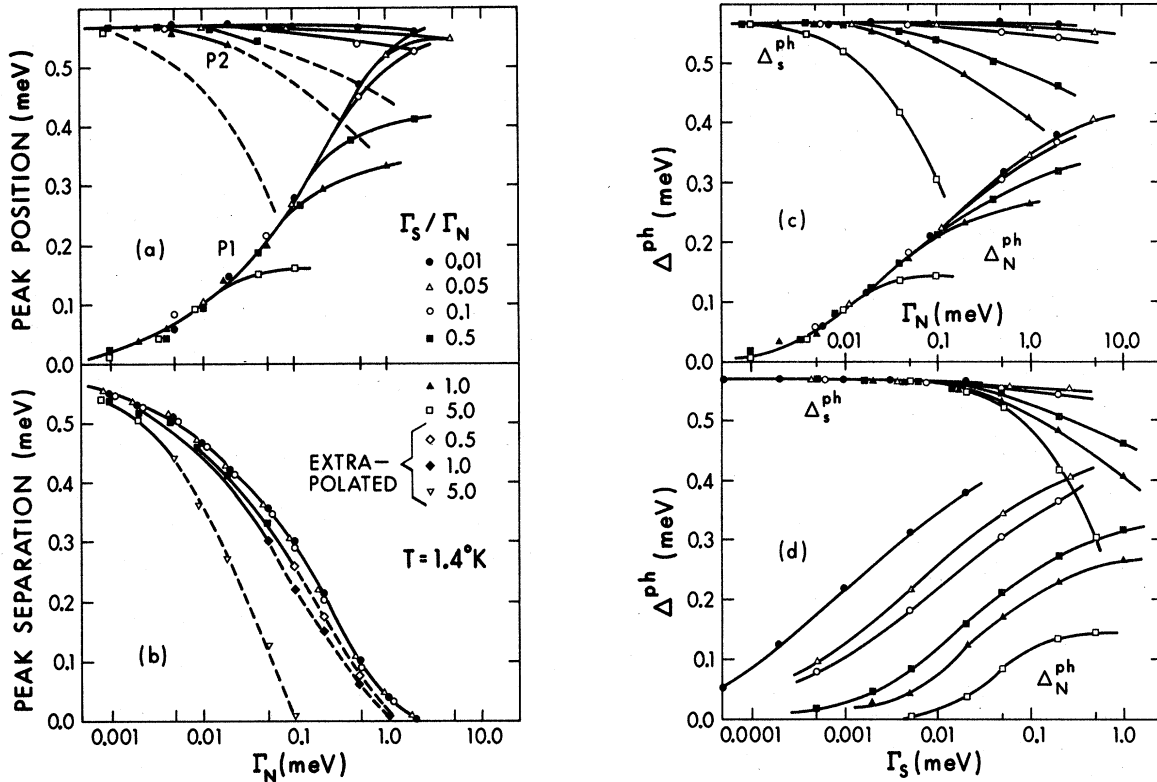
FIG. 3. (a) Self-consistently determined peak positions in the N side of McMillan's density of states for aluminum-tin sandwich as a function of Γ_N. (b) Peak separation in the N side of aluminum-tin sandwich determined from (a) as a function of Γ_N. (c) Self-consistent values of potentials Δ_S^{ph} and Δ_N^{ph} in the N side of aluminum-tin sandwich as a function of Γ_N. (d) The same as (c) but as a function of Γ_S. The properties of the system are weakly dependent on Γ_S, whereas the strong dependence on Γ_N is emphasized in (d).

an Al-I-Sn junction at $T \simeq 1.0$ °K, yielding δ_{S_n} $= 0.038$. A comparison of the calculated and experimental curves for this junction is shown in Fig. 4(a). The approximate density of states for a superconductor was then used in Eq. (7) to calculate the tunnel conductance of a normal-metal–superconductor junction. Comparison with Bermon's calculations[14] for a similar junction, plotted in Fig. 4(b), shows that the conductance values agree within 1%. We conclude that the approximate density of states of (8) is adequate to use in the calculation of the tunnel conductance of a junction formed between a superconductor (or a normal metal) and a proximity sandwich characterized by the McMillan density of states.

Tunneling from Normal Metal into N Side of Proximity Sandwich

A general feature of tunneling from a normal metal into the N side of a proximity sandwich may be observed by considering the experimentally measurable quantity $1 - \sigma(0)$. For tunneling into a BCS superconductor $1 - \sigma(0) \propto 1 - T/T_c \propto \Delta^2$, whereas it increases less rapidly than this with

decreasing temperature just below T_c for tunneling into the N side of a proximity structure and then grows faster as the temperature is lowered. Guyon et al.[5] proposed the empirical relationship $1 - \sigma(0)$ $\propto (1 - T/T_c)^n$, which fitted their data for proximity sandwiches made with zinc and indium-bismuth alloys. They and other observers[15] have obtained n values between 2.3 and 3.0, but their N films were at least 1000 Å thick and it is probably that the electron mean free path was smaller, thus violating one of the conditions of the McMillan model.

In Fig. 5 the behavior of our aluminum-tin samples, in which the slopes range from about 1 to 6, is shown. Slopes of higher value are very difficult to measure because the temperature where the energy gap develops, which is used as the experimental T_c, cannot be measured accurately when $\sigma(0)$ is varying very slowly with temperature.

These results are in good accord with the McMillan model. For weak coupling (small α), the magnitude of Δ_N^{ph} is very small, as may be seen in Fig. 2, and increases slowly with decreasing temperature, producing the same behavior in $1 - \sigma(0)$ until
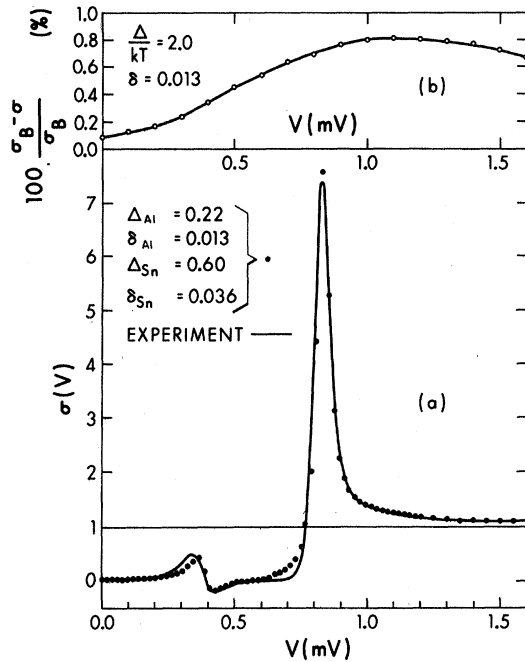
FIG. 4. (a) Normalized tunneling conductance $\sigma(V)$ in the junction Al-I-Sn. Solid line, experimental curve; closed circles, calculation using the smeared BCS density of states with $\Delta_{Al}=0.22$ meV, $\delta_{Al}=0.013$, $\Delta_{Sn}=0.60$ meV, and $\delta_{Sn}=0.036$. (b) Deviation of Bermon's conductance σ_B from the normalized tunneling conductance $\sigma(V)$ between a normal metal and the smeared superconducting density of states ($\delta=0.013$, $\Delta/kT=2.0$).

temperatures near the critical temperature of aluminum are reached; thereafter these quantities both rise rather sharply. For the strong-coupling cases (case c, Fig. 2), Δ_N^{ph} approaches the BCS behavior and so does the experimental slope of $1-\sigma(0)$. We calculated $\sigma(0)$ as a function of temperature for different combinations of Γ_N and Γ_S, using the relationships of the McMillan model. T_c was estimated using Eq. (5) and $1-\sigma(0)$ vs $1-T/T_c$ was plotted logarithmically as shown in Fig. 6. The curvature of these graphs is small and straight lines were readily fitted and their slopes n determined. These n values were plotted as a function of Γ_N for different ratios of Γ_S/Γ_N. Just as for the properties shown in Fig. 3, the value of the slope is independent of Γ_S over a wide range of Γ_N. This important result facilitates the determination of Γ_N (or α/B_N) for experimental samples without the necessity of knowing Γ_S (or B_S). The calculations with McMillan's model for Γ_N between 5.0 and 0.001 meV show that n may vary from 1 (strong coupling) to 25 (weak coupling).

In Fig. 7, $\sigma(V)$ has been plotted as a function of applied voltage for sample $D81$ (with $d_N=115$ Å, $d_S=3150$ Å), together with the curve for tunneling into a BCS superconductor and the curve for the

McMillan model, all at $T/T_c=0.73$. It is immediately clear that the experimental results are vastly different from the BCS results and fit the McMillan model very well, particularly when the effects of a slight error in the determination of the tunnel conductance when the proximity sandwich is just above T_c are considered. In order to obtain the curve for the McMillan model, the values $\Gamma_N=0.047$ meV and $T=2.63$ °K were used, and assuming $B_N=B_S$ and $v_{FN}=v_{FS}$, we obtained $\Gamma_S/\Gamma_N=0.05$. The results are relatively insensitive to the value of Γ_S/Γ_N, T_c is the same as that for the experimental sample, and $\Gamma_N=0.047$ meV fits the slope $n=3.48$ (see Fig. 6), which was determined from a plot like Fig. 5 for sample $D81$.

Tunneling from Superconductor into N Side of Proximity Sandwich

Although tunneling into a proximity structure from a normal metal above 1 °K is clearly distinguishable from that into an ordinary superconductor after some analysis, the normalized conductance for tunneling from a superconductor into a weakly coupled proximity sandwich exhibits the very characteristic multiple-peaked structure shown in Fig. 8(b). This curve was constructed for tunneling at
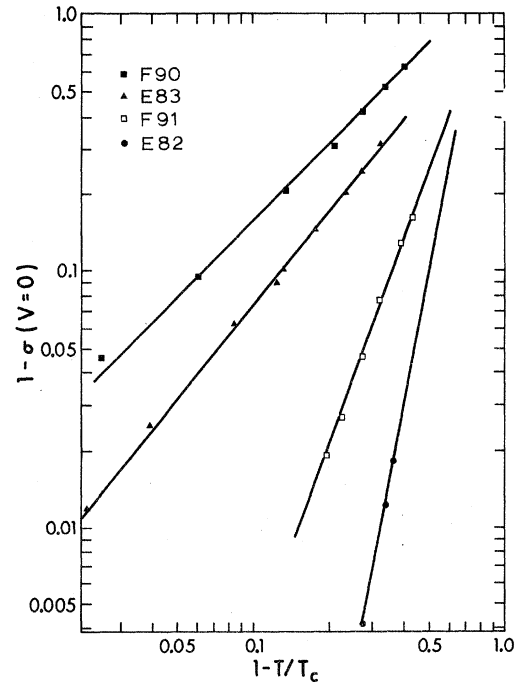

FIG. 5. Experimental dependence of $1-\sigma(V=0)$ on $1-T/T_c$. $\sigma(V=0)$ is the normalized tunneling conductance at zero bias between a normal metal and the N side of aluminum–tin proximity structure. The appropriate experimental values of Γ_N determined from Fig. 6 are ■, $\Gamma_N=1.0$ meV; ▲, $\Gamma_N=0.55$ meV; □, $\Gamma_N=0.05$ meV; ●, $\Gamma_N=0.02$ meV.
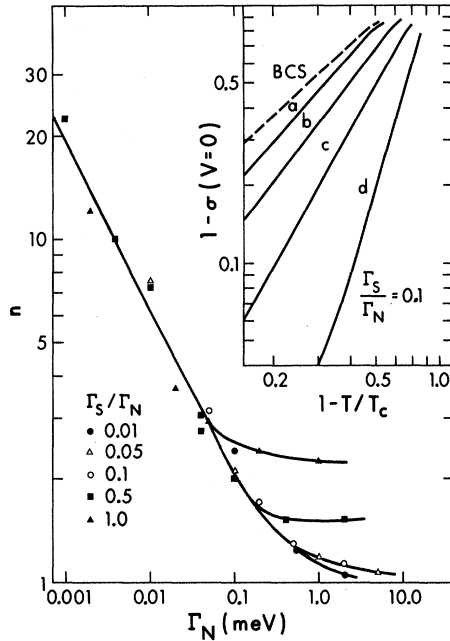
FIG. 6. Calculated values of the exponent n in the empirical expression $1 - \sigma(V=0) \propto (1 - T/T_c)^n$ for tunneling from a normal metal into the McMillan model for aluminum–tin using different values of Γ_S/Γ_N. In the insert the calculated dependence of $1 - \sigma(V=0)$ on $1 - T/T_c$ is shown. Solid curve, McMillan model, $\Gamma_N/\Gamma_S = 0.1$.
(a) $\Gamma_N = 2.0$ meV, (b) $\Gamma_N = 0.5$ meV, (c) $\Gamma_N = 0.2$ meV, (d) $\Gamma_N = 0.05$ meV. Dashed curve, BCS dependence.

1.4 °K between the density of states for aluminum and the McMillan density of states shown in Fig. 8(a). The expected energies of structure are indicated by arrows at $P1\pm\Delta$ and $P2\pm\Delta$. The structure at $P2 - \Delta$ is usually very small because the concentration of thermally excited electrons which contribute most of this peak and the change in the density of states in $P2$ are usually much smaller than in $P1$.

In Fig. 9 an experimental curve (for $d_N = 100$ Å, $d_S = 2260$ Å) is compared with a calculated curve using $\Gamma_N = 0.1$ meV and $\Gamma_S = 0.005$ meV. There are two possible ways of fitting the calculated and experimental curves. From experiment the peak separation can be measured and the resulting Γ_N obtained from Fig. 3(b), or the position of structure $P1$ can be measured (taking account of the influence of the gap of the pure aluminum electrode) and Γ_N can be determined from Fig. 3(a). Structure $P1$ is selected because its sensitivity to Γ_N is higher than that of $P2$. The first method was used in constructing Fig. 9 and values of Δ_S^{ph} and Δ_N^{ph} were estimated from Fig. 3(c). As expected, the fit in insensitive to Γ_S, so that the assumptions $B_N = B_S$ and $v_{FN} = v_{FS}$ are adequate. We then obtain $\Gamma_S/\Gamma_N \simeq d_N/d_S \simeq 0.005$ and $\Gamma_S = 0.005$ meV. The structure on the calculated curve is sharper

than the experimental structure and a better fit to the shape of the structure would be obtained using $\Gamma_S = 0.05$ meV. This discrepancy probably arises because the density of states in the McMillan model rises too rapidly from zero on the low-energy side. Our assumed density of states for aluminum has been shown to produce less sharply peaked structure than experiment [Fig. 4(a)] and adjustment of other parameters in the theory either produces sharper structure or values that are inconsistent with the experimental information.

The temperature dependence of McMillan's peak structure should follow the curves marked by $P1$ and $P2$ in Fig. 2. This dependence is combined in the tunneling experiment with the BCS temperature dependence of the gap edge in the aluminum electrode, to form the temperature dependence of $P1 \pm \Delta$ and $P2 \pm \Delta$. The results of a typical experiment are plotted in Fig. 10. At most temperatures the structure $P2 - \Delta$ was not resolved, but, since there are four structures and only three unknowns
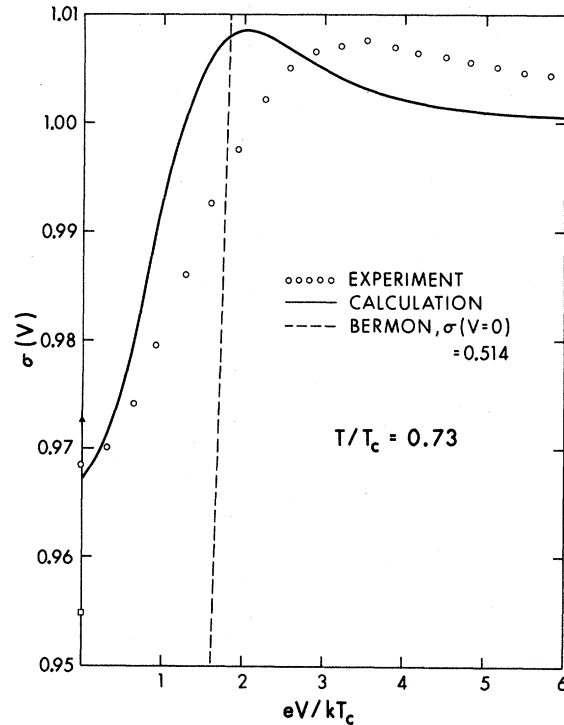

FIG. 7. Normalized tunneling conductance $\sigma(V)$ between a normal metal and an aluminum–tin sandwich.
O, experiment $D81$, $T_c = 3.6$ °K, $d_{Al} = 115$ Å, $d_{Sn} = 3150$ Å. Solid curve, calculated from the McMillan model with $\Gamma_N = 0.047$ meV, $\Gamma_S = 0.0024$ meV, $\Delta_S^{ph} = 0.474$ meV, and $\Delta_N^{ph} = 0.061$ meV. $T = 2.626$ °K and $T/T_c = 0.73$ for both. At zero bias only, the theoretical calculations are included for $\Gamma_S/\Gamma_N = 0.05$ and $\Gamma_N = 0.04$ meV ($\blacktriangle$), $\Gamma_N = 0.06$ meV ($\square$). For comparison, part of the Bermon conductance σ_B for the same T/T_c is shown by dashed line. $\sigma_B(V=0) = 0.514$.
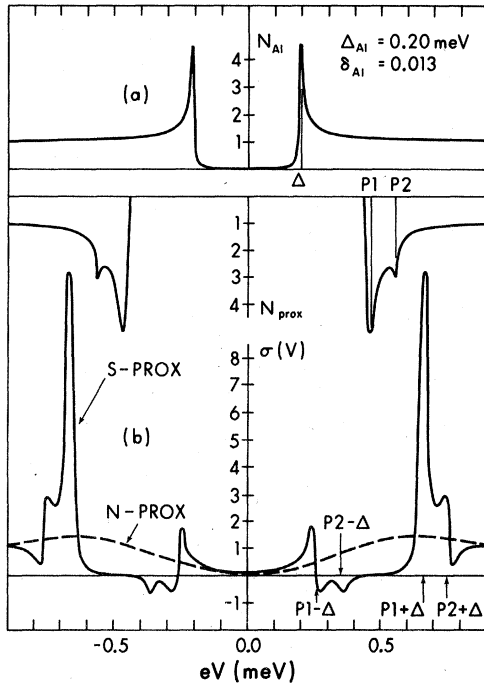
FIG. 8. Illustration of the occurrence of multiple-peak structure in the tunneling conductance between an ordinary superconductor and an aluminum–tin proximity sandwich. (a) Normalized densities of states in the superconducting aluminum N_{Al} (characterized by Δ_{Al} = 0.20 meV, δ_{Al} = 0.013) and proximity sandwich N_{prox} (characterized by Γ_S = 0.025 meV, Γ_N = 0.5 meV, Δ_S^{ph} = 0.56 meV, and Δ_N^{ph} = 0.31 meV). When voltage is applied, the densities of states shift on the energy scale. (b) Resulting calculated tunneling conductance at 1.4 °K (solid line). Expected structures at $P1 \pm \Delta$ and $P2 \pm \Delta$ are indicated by arrows. For comparison the tunneling conductance between a normal metal and the same proximity sandwich at the same temperature is also plotted (dashed line).

$P1$, $P2$, and Δ, it is possible to calculate the unknowns at each temperature from three structures and reconstruct the position of the fourth or check the consistency of the method where all four structures are resolved. Also Δ, the gap of the aluminum electrode, can be compared with the temperature variation of a BCS gap with $T_c = 1.7$ °K as has been done in the lower part of Fig. 10. Remarkably good agreement is obtained. The values of $P2$ from the McMillan-model calculations lie within the scatter of the experimental values, whereas the values of $P1$ lie about 0.025 meV lower than the experimental curve at all temperatures.

Tunneling into the S side of these aluminum–tin sandwiches may yield information that, combined with the present data, would provide a more definitive comparison with theoretical models. Also experiments with thicker films would be interesting, but it will then be more difficult to satisfy the

condition $l > d$ necessary for the McMillan model. It would be valuable to have a model that would connect the de Gennes[10] assumption of the dirty limit in thick S films with McMillan's assumptions in thin N films.

Other experimenters have possibly seen some evidence of the multiple peaks in thicker films. Claeson et al.[15] observed structure with an aluminum-lead sandwich that they assigned to the superconducting properties of the contacts. It disappeared at lower temperatures, possibly because the smaller peaks are more difficult to resolve there. Adkins and Kington[2] observed "unexplained dips in the density of states above the gap and structure at zero voltage" on the tunneling conductance from aluminum into a copper-lead proximity sandwich at 1.25 °K. This is just the kind of structure to be expected if the aluminum was superconducting and their copper-lead sandwich had a clean interface with a high α. Freake and Adkins[3] have observed broad multiple peaks in normal-metal prox-
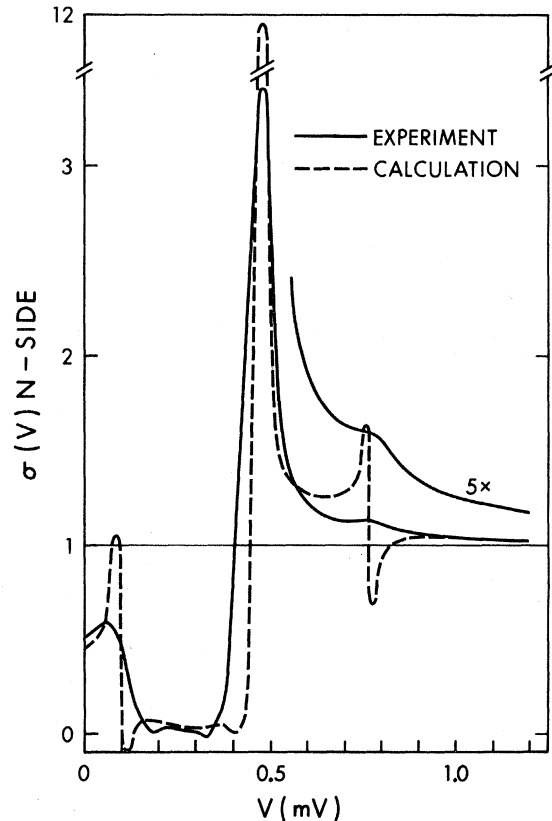

FIG. 9. Comparison of experimental and theoretical normalized conductance for tunneling from superconducting aluminum into aluminum–tin proximity sandwich. Solid curve, experiment $E82$, $T = 1.4$ °K, $d_{Al} = 100$ Å, and $d_{Sn} = 2260$ Å. Dashed curve, calculated, $\Gamma_S = 0.005$ meV, $\Gamma_N = 0.1$ meV, $\Delta_S^{ph} = 0.56$ meV, and $\Delta_N^{ph} = 0.22$ meV. Aluminum electrode from which the tunneling was done is characterized by $\Delta_{Al} = 0.20$ meV and $\delta = 0.013$.
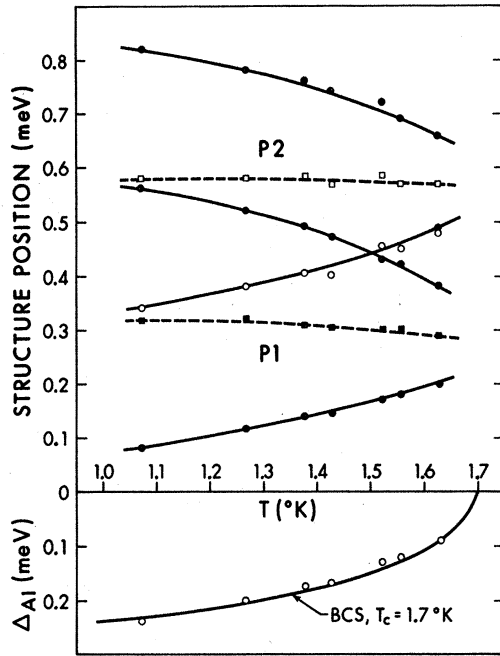
FIG. 10. Temperature dependence of the peak positions. ●, experimental points corresponding to $P1 - \Delta$, $P1 + \Delta$, and $P2 + \Delta$, $E82$, $d_{Al} = 100$ Å, $d_{Sn} = 2260$ Å. O, calculated positions of $P2 - \Delta$ using the experimental points. Note the consistency of the results at 1.63 °K, where calculated and experimental points coincide. $P1$ (■) and $P2$ (□) positions calculated from experimental points. In the lower graph the gap of the aluminum electrode is shown from which tunneling into the proximity structure was performed (O) as calculated from experimental points in the upper part. For comparison the BCS temperature variation of a gap is included.

imity tunneling done at $T \simeq 0.06$ °K and Hauser[4] reported structure near Δ for lead when tunneling into an aluminum-lead sandwich.

Dependence of Data on α and Thickness

In Table I the Γ_N values determined from experimental data by the three different methods discussed earlier are compared. Only the peak-position method was used for the samples of Sec. III because neither T_c nor the position $P2$ could be accurately determined for these weakly coupled (low-α) sandwiches. The α values were determined using Eq. (4) and putting $B_N = 2$, which may be an assumption of limited accuracy because B_N probably rises rapidly above this value if the condition $l_N \gg d_N$ is not fulfilled. We do have some evidence that $l_N \simeq 2d_N$ for these films from resistivity measurements on thin evaporated aluminum films that we have fitted to the Sondheimer[16] calculations treating l as a parameter. The difference among the α values determined by the three methods arises partly because bulk values of ω_c and λ for aluminum were used in the self-consistent calculations, whereas it is well known that different values apply to thin films.[17] These bulk values mainly affect the relationship between n and Γ_N for the McMillan model and thus affect the reliability of the slope method of determining Γ_N because of its dependence on T_c. However, it is clear that α decreases systematically as the amount of oxidation at the interface increases, being in about the ratio 80:20:1 for the samples of Secs. I, II, and III, respectively. This range of α values was achieved by creating the following conditions during the time interval Δt between the evaporation of the aluminum and tin.

TABLE I. Transmission probability α and Γ_N as a function of the oxidation conditions for Al-Sn proximity sandwiches at 1.4 °K.

Section	Junction[a]	d_N (Å)	d_S (Å)	$P2 - P1$ (meV)	Γ_N (meV)	α $(B_N = 2)$	$P1$ (meV)	Γ_N (meV)	α $(B_N = 2)$	n	(meV)	$(B_N = 2)$
				Peak separation $P2 - P1$			Peak position $P1$			Slope n		
	A84	105	2300	0.10	0.5	0.066	0.65	1.0	0.13			
	A85	123	1030				0.65	1.0	0.16			
I	B87	113	397	0.085	0.6	0.085	0.45	0.5	0.072			
	C92	39	790				0.56	2.0	0.097	1.01	2.0	0.097
	C93	266	2370				0.49	0.7	0.23	1.37	0.4	0.13
	D81	115	3150	0.20	0.22	0.032	0.30	0.13	0.043	3.48	0.047	0.0078
	E82	100	2260	0.26	0.15	0.018	0.27	0.10	0.034	5.20	0.02	0.0026
II	E83	67	2480	0.17	0.34	0.028	0.52	0.7	0.044	1.17	0.55	0.046
	F90	42	783	0.20	0.22	0.011	0.50	0.8	0.041	1.05	1.0	0.051
	F91	221	821	0.39	0.025	0.0068	0.29	0.12	0.033	2.81	0.05	0.014
	G89	105	910				0.14	0.02	0.0026			
III	H53[b]	89	1450				0.08	0.009	0.0010			
	H54[b]	117	2120				0.10	0.01	0.0015			

[a] Junctions designated by the same letter were prepared at the same time on the same substrate.

[b] These specimens were exposed to room atmosphere before measurement.

Section I samples. Pressure ~ 2×10^{-7} Torr, $\Delta t \simeq 1$ min, and a shield around the sample was held at liquid-nitrogen temperatures.

Section II samples. Pressure ~ 5×10^{-7} Torr, $\Delta t \simeq 1$ min.

Section III samples. Specimen chamber isolated from pumps, pressure $\gg 10^{-7}$ Torr for $\Delta t \simeq 10$ min. All pressures were read on a cold-cathode ionization gauge.

The process of trying to control α is very complex and cannot be done with precision. In a vacuum of 3×10^{-6} Torr a monolayer strikes a clean surface in about 1 sec, so one cannot hope for an ideally clean surface, especially on aluminum, which oxidizes readily. Absorbed layers are partially penetrated by the next metal that is evaporated, so that interface properties will depend on many factors, including the specific metals involved.[18]

Finally, it may be noted from Table I that the measurable parameters depend on the thickness d_N in accord with the McMillan model. Samples from different sections cannot be compared because the α dependence masks the thickness effect. Samples prepared at the same time provide the most striking comparison; for example, the E samples have $d_N(E82)/d_N(E83) = 1.5$, whereas from the peak-separation method $\Gamma_N(E83)/\Gamma_N(E82) = 1.55$. As expected, the properties are only slightly dependent on the thickness of the tin film.

CONCLUSION

The tunneling characteristics of junctions between aluminum and the aluminum side of proximity sandwiches formed by evaporated films of aluminum and tin have been measured. The coupling of the proximity films has been limited by allowing slight oxidation at the interface, and the results for these weakly coupled proximity sandwiches agree closely with the predictions of the McMillan model of the superconducting proximity effect.

The junction conductance at zero bias when tunneling from normal aluminum has been compared with the empirical expression $1 - \sigma(0) = \text{const} \times (1 - T/T_c)^n$. Values of n from 1 to 6 have been obtained. The McMillan model predicts the observed magnitude of $\sigma(0)$ and very nearly this temperature dependence, although for the higher n values the experimental data fit the empirical law somewhat better than the model calculations do. The measured conductance as a function of voltage fits the McMillan model very well.

When the aluminum is superconducting, a multi-peaked conductance curve is observed and compares well in some detail with the predictions of the McMillan model. The positions of the peaks and their variation with temperature as well as their dependence on the proximity film coupling and thickness of the normal (aluminum) film have all been compared with theory. Those discrepancies that exist may be largely a result of applying calculations using properties of bulk aluminum to experiments with thin films. The McMillan theory predicts sharper peaks than the observed ones, and that appears to be due to a density of states in the proximity model that rises too sharply from zero.

ACKNOWLEDGMENTS

*Research supported in part by the National Research Council of Canada.

[1] W. L. McMillan, Phys. Rev. **175**, 537 (1968).

[2] C. J. Adkins and B. W. Kington, Phys. Rev. **177**, 777 (1969).

[3] S. M. Freake and C. J. Adkins, Phys. Letters **29A**, 382 (1969).

[4] J. J. Hauser, Physics **2**, 247 (1966).

[5] E. Guyon, A. Martinet, S. Mauro, and F. Meunier, Physik Kondensierten Materie **3**, 123 (1966).

[6] J. S. Shier and D. M. Ginsberg, Phys. Rev. **147**, 384 (1966).

[7] J. D. Leslie, J. T. Chen, and T. T. Chen, Can. J. Phys. **48**, 2783 (1970).

[8] J. L. Miles and P. H. Smith, J. Electrochem. Soc. **110**, 1240 (1963).

[9] M. Hansen, *Constitution of Binary Alloys* (McGraw-Hill, New York, 1958).

[10] P. G. de Gennes, Rev. Mod. Phys. **36**, 225 (1964).

[11] The correct integration limits are Δ^{ph} and $[\omega_c^2 + (\Delta^{\text{ph}})^2]^{1/2}$, but the contribution to the integrals is zero, between zero and Δ^{ph}, and $\Delta^{\text{ph}} \ll \omega_c$, so the limits may be written 0 and ω_c; thus $B = \omega_c^N$, $D = \omega_c^S$, and $A = C = 0$.

[12] A. B. Kaiser and M. J. Zuckermann, Phys. Rev. B **1**, 229 (1970).

[13] J. Bardeen, L. N. Cooper, and J. R. Schrieffer, Phys. Rev. **108**, 1175 (1957).

[14] S. Bermon, National Science Foundation Technical Report No. 1, 1964 (unpublished) (Grant No. NSF - GP 1100).

[15] T. Claeson, S. Gygax, and K. Maki, Physik Kondensierten Materie **6**, 23 (1967).

[16] E. H. Sondheimer, Advan. Phys. **1**, 1 (1952).

[17] M. Strongin, O. F. Kammerer, and A. Paskin, Phys. Rev. Letters **14**, 945 (1965).

[18] R. M. Handy, Phys. Rev. **126**, 1968 (1962).